

# Lubricated friction and volume dilatancy are coupled

A. Levent Demirel

*Koç University, Chemistry Department, Sariyer 80910, Istanbul, Turkey*

S. Granick

*University of Illinois, Materials Science & Engineering Department, Urbana, Illinois 61801*

(Received 1 April 2002; accepted 18 June 2002)

Dilation (expansion of film thickness) by  $\sim 0.1 \text{ \AA}$ , which is less than one-tenth of the width of confined fluid molecules, was observed when confined films crossed from the resting state ("static friction") to sliding ("kinetic friction"). These measurements were based on using piezoelectric bimorph sensors possessing extremely high resolution for detecting position changes, during the course of sliding molecularly thin films of squalane, a model lubricant fluid, between atomically smooth single crystals of mica. Detailed inspection of energy balance shows that the dilation data and the friction forces satisfied energy conservation of identifiable energies at the slip point, from static to kinetic friction. This shows experimentally, for the first time to the best of our knowledge, a direct coupling between friction forces and decrease in the mean density of the intervening molecularly thin fluid. © 2002 American Institute of Physics. [DOI: 10.1063/1.1499476]

## INTRODUCTION

In 1885, Reynolds coined the word "dilatancy" to refer to the increase of volume of a granular medium in response to a change in the relative positions of the grains and added that dilatancy is not observed with the known (bulk) fluids.<sup>1</sup> Since then this concept has been associated with granular materials, but not with fluids. It is true that fluids of course possess some compressibility; if not, sound waves would not travel through them. Nonetheless, in the analysis of fluid dynamics, it is a fundamental tenet that changes in density upon deformation are insignificant for the purposes of such analysis.<sup>2</sup> Bulk fluids are, for practical purposes of analyzing fluid flow, "incompressible."

However, recent research on liquids confined to molecularly thin spacings between rigid surfaces reveals the profound effects of molecular discreteness of simple liquids on friction.<sup>3–6</sup> Much friction behavior of confined fluids so closely resembles that of dry granular materials such as sand and powder<sup>7,8</sup> that an observer could not distinguish between the two if the experiment were performed in a black box. This phenomenological similarity can be understood on physical grounds to reflect the fact that the structural organization of fluid molecules at the solid–liquid interface is so dominated by the packing and crowding of molecules at a rigid, unyielding boundary.<sup>9</sup>

In these jammed systems, the existence of dilatancy in boundary lubrication may be intuitively anticipated. In a pioneering investigation based on computer simulation, Thompson, Grest, and Robbins found by molecular dynamics (MD) simulation that film thickness increased when shear was induced relative to the resting state.<sup>10</sup> But relevance to laboratory experiments was unclear because the effective rates of shear exceeded, by several orders of magnitude, time scales of laboratory experiments. From another point of view entirely, Schoen, Diestler, and Cushman employed Monte Carlo simulations to predict quasistatic shear-induced defor-

mations, and also predicted that shear would produce increased film thickness.<sup>11</sup> Shear dilatancy in simple fluids in the bulk state but at very high shear rate was also investigated by Woodcock using molecular dynamics simulations.<sup>12</sup> It was predicted based on a model of shear melting.<sup>6</sup> It can also be inferred from the observation that small-amplitude vertical modulations of the spacing between sliding solid boundaries modify the friction of lubricated surfaces.<sup>13–15</sup> From all of these points of view this phenomenon is anticipated in principle.

Yet the experimental challenge of measuring dilatancy in fluids is apparent when one considers that the magnitude is known, from study of granular beads, to be on the order of one-tenth of the mean particle size.<sup>7</sup> Recently this research group measured for the first time the shear-induced dilation of several molecularly thin fluids of different types and sizes (water, squalane, octamethylcyclotetrasiloxane, and a block copolymer); in each case, the observed amount of dilation was on the order of one-tenth of the molecular dimension, although the actual sizes of these molecules differed.<sup>16</sup> Note that when we use the term dilatancy in this paper, its meaning is different from that used by Israelachvili and coworkers to denote the expansion of film thickness when sliding induces more fluid to enter the gap between two sliding surfaces.<sup>17</sup> In that case the amount of fluid increases but its density does not.<sup>17</sup> In the present problem, we believe that the amount of fluid is fixed but its density decreases.<sup>16</sup> In this respect, the dilatancy of concern here is akin to the dilatancy of sand when one walks on it.

## EXPERIMENT

The measurements employed a surface force apparatus (SFA) modified to measure shear forces and normal forces concurrently.<sup>16</sup> A schematic representation of the apparatus is shown in Fig. 1. A droplet of squalane (Aldrich) was confined in a dry air environment between two atomically

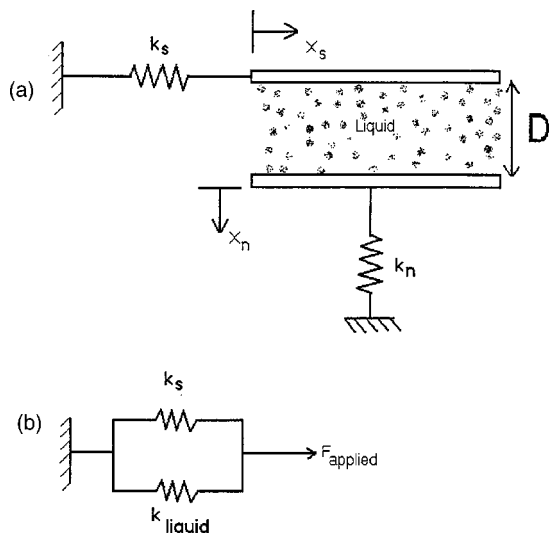


FIG. 1. Schematic drawing of the experimental apparatus. (a) The liquid is confined between two solid surfaces at a separation of  $D$ . The top surface is connected to a spring of stiffness  $k_s$  in the horizontal direction (shear direction) and the bottom surface is connected to a spring of stiffness  $k_n$  in the vertical (orthogonal) direction. The shear displacement,  $X_s$ , is the same for the horizontal spring and the confined liquid. The orthogonal displacement  $X_n = X_{\text{elastic}} + \Delta D$  as discussed in the text. (b) Applied force,  $F_{\text{applied}}$ , acts on the parallel arrangement of the horizontal spring  $k_s$  and the confined liquid of stiffness  $k_{\text{liquid}}$ .

smooth mica surfaces and normal pressure was applied to push the surfaces to the known point of “hard wall” repulsion<sup>18</sup> at a surface separation  $D$ , of  $16 \pm 1 - 2 \text{ \AA}$  (measured by multiple beam interferometry). At this point the curved cylinders of the SFA apparatus became flattened at their apex to form parallel plates with dimension of approximately  $40 \mu\text{m}$  and the squalane film responded elastically to small values of applied shear force.

This system displays a “stick–slip” transition between static and kinetic friction. To measure friction, the top surface was attached to two piezoelectric bimorphs that are represented in Fig. 1(a) as a spring of stiffness  $k_s = 68\,400 \text{ N/m}$ . A sinusoidal shear force  $F_{\text{applied}}$  was applied to one of the bimorphs and the resulting motion was measured using the second bimorph. Because the displacement of the bimorphs is equal to the shear displacement of the liquid  $X_s$ , the two can be represented as a parallel arrangement of springs of stiffness  $k_s$  and  $k_{\text{liquid}}$  in response to the applied force  $F_{\text{applied}}$ , as in Fig. 1(b), and discussed in more detail elsewhere.<sup>4</sup> The component of  $F_{\text{applied}}$  that acts on the liquid is then given by  $F_{\text{liquid}} = F_{\text{applied}} k_{\text{liquid}} / (k_{\text{liquid}} + k_s)$ .

To measure dilation, the piezoelectric setup was analogous, but mounted at right angles to the direction of sliding. In this case the spring constant  $k_n$  resisting dilation was  $1000 \text{ N m}^{-1}$  and the voltage constant, displacement per output voltage, was  $0.0054 \text{ \AA } \mu\text{V}^{-1}$ . The output voltage was measured using a digital lock-in amplifier (Stanford Research Systems SR850) at  $\mu\text{V}$  sensitivity, giving a displacement sensitivity of  $\sim 0.0054 \text{ \AA}$  above the background electrical noise of  $\sim 5 \mu\text{V}$ . A detailed consideration of the calibration of piezoelectric bimorphs for small displacements was presented previously.<sup>16</sup> In the present context, we emphasize

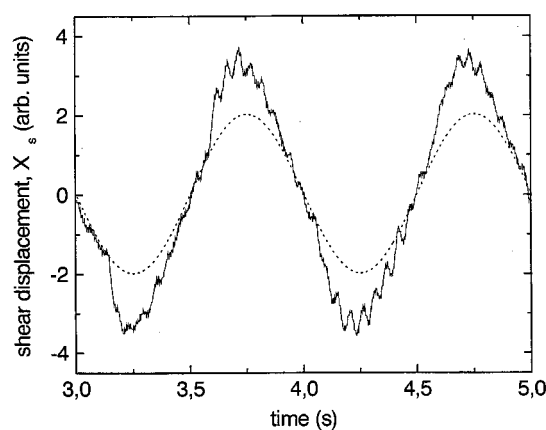


FIG. 2. The dotted line shows the elastic shear response when the force acting on the confined liquid,  $F_{\text{liquid}}$ , is less than the yield force,  $F_{\text{yield}}$ . The solid line shows two periods of the measured data in the stick-slip regime, when  $F_{\text{liquid}}$  is slightly larger than  $F_{\text{yield}}$ .

again that the method records changes of displacement rather than magnitude. It would not be suited to measure the absolute film thickness, but is very sensitive to recording changes in it.

To mitigate the effect of the background electrical noise, we took advantage of a slight misalignment between the top and bottom surfaces such that the direction of shear force was applied at a slight angle off the parallel direction,  $\theta_m \leq 2.5^\circ$ . A shear displacement of amplitude  $X_s$  in the liquid therefore also produced a displacement of the confined film in the orthogonal (normal) direction with amplitude  $X_n = X_s \sin \theta_m$ , usually amounting to a voltage of  $44 \mu\text{V}$  between the two bimorphs in these experiments. As this value much exceeded the background noise, the small voltage changes that reflected dilation  $\Delta D$  (the increase in the surface separation  $D$ ) at the transition from static to kinetic friction could easily be measured. Below we discuss how to separate dilation (the item of interest), from this periodic orthogonal displacement of amplitude  $X_n$  in the laboratory frame of reference.

## RESULTS

Experiments were usually performed by applying sinusoidal shear forces periodically at  $1 \text{ Hz}$ . When the amplitude of the applied force acting on the liquid ( $F_{\text{liquid}}$ ) was smaller than the yield force of the elastically responding squalane film, then the resulting shear displacement was also sinusoidal and had an amplitude  $X_s = F_{\text{liquid}} / k_{\text{liquid}} = F_{\text{applied}} / (k_s + k_{\text{liquid}})$ , as shown schematically by the dotted line in Fig. 2. When  $F_{\text{liquid}}$  exceeded the yield force, the squalane film ruptured and the elastic stiffness of the film decreased significantly. At the time of this rupture,  $X_s = X_{\text{yield}}$ ,  $F_{\text{applied}} = (k_s + k_{\text{liquid}}) X_{\text{yield}}$ , and  $F_{\text{liquid}} = F_{\text{yield}} = k_{\text{liquid}} X_{\text{yield}}$ . Just after the rupture,  $k_{\text{liquid}}$  was negligible with respect to  $k_s$ . So  $F_{\text{applied}}$  became much larger than the restoring force  $k_s X_{\text{yield}}$  and the top surface slid on top of the bottom surface. The resulting shear displacement was sinusoidal up to the yield point and then increased sharply as shown by the solid line in Fig. 2.

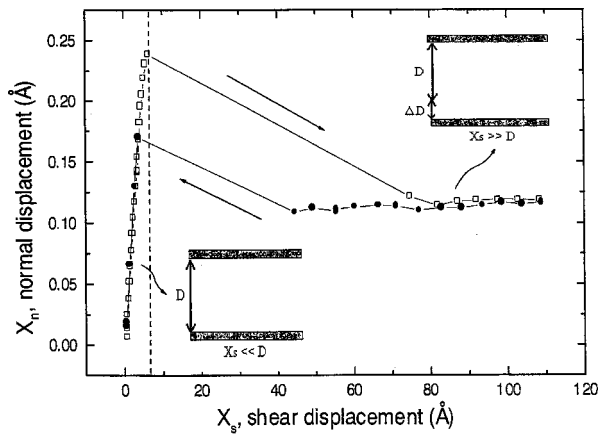


FIG. 3. Time-averaged data showing the changes of vertical displacement of the bottom surface (in the laboratory frame of reference) as a function of shear displacement of the top surface,  $X_s$ , for a film of squalane, 16 Å thick, confined between parallel sheets of mica. The linear dimension of the contact zone, 40 μm, greatly exceeded the shear amplitude. Open squares represent the data taken in the direction of increasing  $X_s$  and the filled circles were taken in the direction of decreasing  $X_s$ . The vertical dashed line separates the elastic response regime (static friction; sticking region) from the regime of kinetic sliding. Insets show sketch of the surface separation in the stick regime (thickness  $D$ ) followed by dilation (thickness  $D + \Delta D$ ) in the slip regime.

The condition for stick–slip transition,  $F_{\text{applied}} > (k_s + k_{\text{liquid}})X_s$ , cannot only be achieved by increasing  $F_{\text{applied}}$  and making  $F_{\text{liquid}} > F_{\text{yield}}$ . Alternatively, even if the applied force is constant,  $k_{\text{liquid}}$  can decrease because of dilation,  $\Delta D$ , and the condition can be satisfied. Viscoelasticity of confined liquids has been shown to depend strongly on the degree of confinement, namely on the separation of confining solid surfaces  $D$ .<sup>3–6,18,19</sup> In this study, we applied a constant force  $F_{\text{applied}}$  to the system (bimorphs+liquid) such that  $F_{\text{liquid}}$  was slightly larger than  $F_{\text{yield}}$  to keep the response in the stick–slip regime (solid line in Fig. 2) and we analyzed stick–slip transition in each cycle. We took advantage of fluctuations that occur in raw waveforms and friction forces under these conditions:<sup>20</sup> we could easily determine the yield points in the raw waveforms and relate the change in the yield force to dilation and kinetic friction.

Although the main point of this communication is to analyze the fluctuations of the yield point and the corresponding fluctuations in the dilation that characterized repeated measurements, the nature of time-averaged data is illustrated in Fig. 3. One sees that the amplitude of the periodic orthogonal displacement in the laboratory frame of reference  $X_n$  increased steeply with increasing amplitude of shear displacement  $X_s$  up to the point of slip, then decreased discontinuously to a constant level in the regime of kinetic sliding. In addition, one sees that the hysteresis that we studied elsewhere, when the amplitude of shear displacement was first raised and then lowered,<sup>19</sup> was also observed as concerns orthogonal displacement. This suggests that orthogonal displacement also reflects changes in the viscoelasticity of the confining film.

In the regime of kinetic sliding, a system undergoes a stick–slip transition twice during each period of oscillatory sliding force: from “stick” to “slip” in each half-cycle of

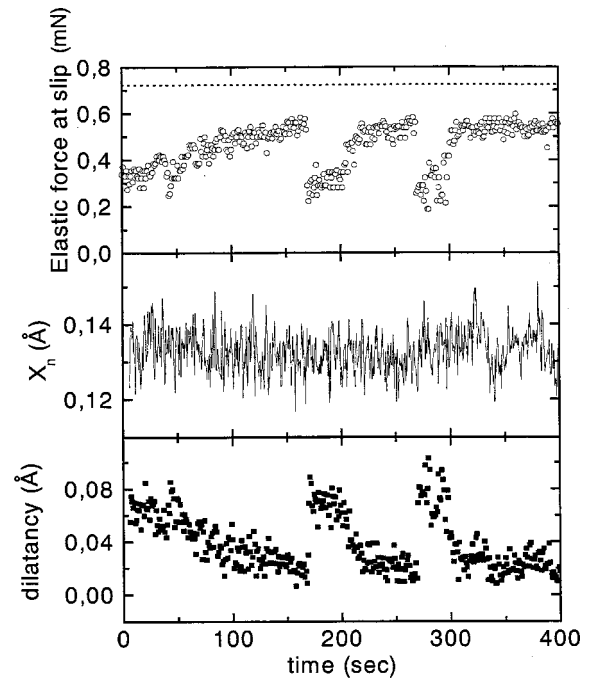


FIG. 4. An extended time series of repetitive measurements made at 1 Hz for 400 s. Top panel: The yield forces, from stick to sliding, during the up cycles of periodic oscillation. The dashed line shows the peak force applied. Middle panel: The vertical displacements of the bottom surface plotted against time. Bottom panel: Dilatancy, calculated from Eq. (1) as described in the text.

applied force, then back to “stick” when the sliding surfaces come to rest at peak displacement during the half-cycle. The orthogonal displacement  $X_n$  can be written as the sum of two contributions:

$$X_n = X_{\text{elastic}} + \Delta D, \quad (1)$$

where  $X_{\text{elastic}} = X_{s(\text{at slip})} \sin \theta_m = X_{\text{yield}} \sin \theta_m$  comes from misalignment of top and bottom surfaces without a change in the film thickness and dilation  $\Delta D$  is the change in the film thickness. The conceivable change of film thickness during kinetic sliding ( $\Delta D_{\text{sliding}}$ ) and the change in the film thickness at the slip point ( $\Delta D_{\text{slip}}$ ) are the two possible contributions to  $\Delta D$ . If a system slides at constant velocity,  $\Delta D_{\text{sliding}}$  can reasonably be taken to be negligible. This is the case in our system because the slip starts close to the peak of the applied force and continues at constant velocity after accelerating in a very short time interval. This assumption is also justified by observations that for granular materials the orthogonal displacement reaches its maximum before the maximum horizontal velocity, over a sliding distance comparable to the size of a particle, and is independent of the drive velocity.<sup>7,8</sup> Dilatancy can then be written as  $\Delta D \cong \Delta D_{\text{slip}} = X_n - X_{\text{elastic}}$ .

An extended time series of repetitive measurements made at 1 Hz for 400 s in the stick–slip regime of the hysteresis loop is summarized in Fig. 4. The shear response was acquired by a storage digital oscilloscope (LeCroy), cycle by cycle, and the orthogonal displacement  $X_n$  was measured simultaneously by lock-in amplifier. The top panel in Fig. 4 shows the time series of static friction, the yield point at which the system passed from “stick” to “slip” with increas-

ing force in one direction. The dotted line, the peak applied force during the oscillation, always exceeded this. The yield forces fluctuated with time with long-lived correlations between repeated cycles. The pattern was a gradual increase in time punctuated by an abrupt decrease to the starting point, in this case twice, once at  $t = 169$  s and again at  $t = 269$  s. We have analyzed similar data elsewhere in detail<sup>20</sup> and attributed these memory effects to the fact that the oscillation period was much shorter than the relaxation time of the molecules to equilibrium. Related measurements, leading to the conclusion that friction traces can exhibit chaotic behavior, were also made by Drummond and Israelachvili.<sup>21</sup> The middle panel in Fig. 4 shows simultaneous measurements of orthogonal displacement. The dilatancy, calculated from the discussion of the previous paragraph, is shown in the bottom panel of Fig. 4.

The dilatancy fluctuations, in the range 0.02–0.08 Å, mainly reflect differences between the yield points from stick to slip. The magnitude of dilatancy decreased during time intervals when the film was stiffening and conversely increased abruptly when the films softened. Unlike cases of steady sliding where an increase of film thickness is believed to reflect suction of additional fluid into the film, without change of density,<sup>17</sup> we believe that the dilatancy reported here actually represented density changes. The key point is that the periodic dilation was too rapid to allow equilibration of fluid within the confined space with the reservoir of fluid outside. Dilation was observed twice during each cycle of periodic shear, twice each second in the present experiments. Consider the fact that the linear dimension of the contact zone was  $\approx 10 \mu\text{m}$ , about  $10^4$  times larger than the thickness. When one considers the known viscosity enhancement of liquids when they are confined, which has been much studied,<sup>3–6</sup> it is evident that times much exceeding the experimental period would be required for fluid of this viscosity to enter and leave the gap so rapidly.<sup>16</sup> The observed rapid occurrence of dilation during periodic sliding, which occurred abruptly at the point of passage from rest to kinetic sliding, signifies that the average density of fluid, within the gap, must have been altered. (Note that this conclusion, which may appear counterintuitive, also emerged from prior computer simulations.<sup>10–12</sup>)

## ANALYSIS

We now postulate, and compare to this data, the hypothesis that the physical connection between the dilatancy, the yield force of the lubricant film, and the friction force after slip can be understood by considering the energy balance between the applied power, elastic energy per time ( $t$ ) at the yield point, the energy per time needed for sliding, and the additional potential energy per time to cause dilation from thickness  $D$  by deflecting a spring of stiffness ( $k_n$ ):

$$\begin{aligned} F_{\text{liquid}}(dX_s/dt) + F_{\text{yield}}(dX_{\text{yield}}/dt) \\ = F_{\text{sliding}}(dX_{\text{sliding}}/dt) + k_n D(dD/dt). \end{aligned} \quad (2)$$

By using this concept of energy conservation at the slip point and the dilation data of Fig. 4 (bottom panel), which was obtained by the analysis of stick–slip transition in each

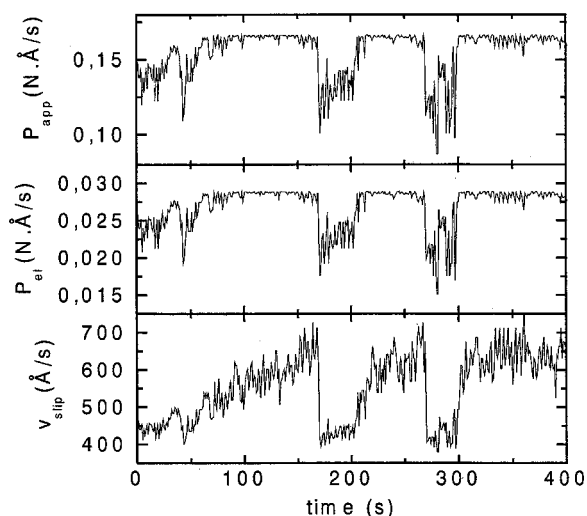


FIG. 5. Top panel: The applied power at the yield point,  $P_{\text{app}}$ , plotted as a function of time. Middle panel: The elastic power at the yield point,  $P_{\text{el}}$ , plotted as a function of time. Bottom panel: The velocity after slip.

cycle, we could successfully fit the friction force that was obtained by the analysis of the fundamental frequency component and decreased linearly with velocity in stick–slip regime close to the transition as we now discuss.

The first term in Eq. (2) is the instantaneous applied power,  $P_{\text{app}}$ , at the yield point. Because of the fluctuations of yield point, applied power at yield also fluctuated from one period to the next as shown in the top panel of Fig. 5. The second term in Eq. (2), the instantaneous elastic power  $P_{\text{el}}$ , was measured directly from the raw waveforms of shear voltage versus time (we have shown elsewhere examples of such data<sup>19</sup>), and is plotted as a function of time in the middle panel of Fig. 5. The contributions of the apparatus response and the film were calculated separately based on the relative stiffness of the two using calibration methods described elsewhere.<sup>19</sup> In regions where dilation decreased with time,  $P_{\text{app}}$  and  $P_{\text{el}}$  were relatively constant. This is because  $dX/dt$  decreased as  $F$  increased. Based on the energy conservation expression and the steady state response,  $P_{\text{app}}$  and  $P_{\text{el}}$  are also expected to be constant in regions where dilation was constant. The data for  $P_{\text{app}}$  and  $P_{\text{el}}$  in these regions were more scattered due to difficulty in determining the slip points on waveforms. The drop in instantaneous power was sharp, more rapid than the sampling interval of 0.002 s, and coincided with sharp changes in velocity and dilation. The subsequent slower rise was accompanied by increase in velocity and decrease in dilation, but the magnitude of these changes was less than for the reverse transition. We tentatively attribute these observations to the sudden formation and gradual growth of seed elastic regions within the confined film.

The sliding velocity,  $V_{\text{sliding}} = dX_{\text{sliding}}/dt$ , was calculated assuming that the sliding surface moved uniformly from the time of slip until it reached the maximum possible displacement for the given applied force. At the maximum displacement the surfaces stuck again and elastic response in the opposite direction was observed. The velocities calculated in this way are comparable in magnitude to the veloci-

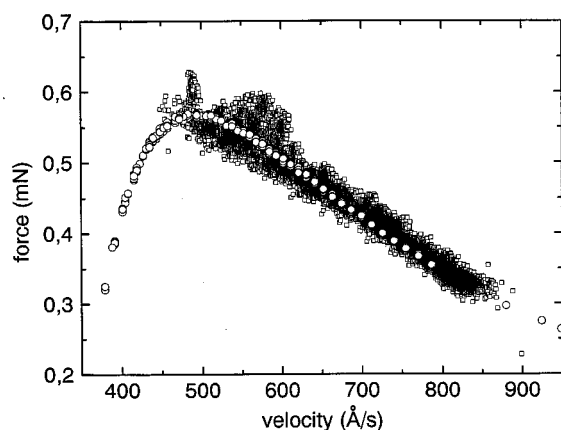


FIG. 6. Comparison of the velocity dependence of the viscous force during sliding. The open squares were calculated from the out of phase component of the stick-slip response as described in the text. The open circles represent  $F_{\text{sliding}}$  in Eq. (2) which was calculated using the dilation data of Fig. 2 and a constant value of  $8 \mu\text{s}$  for  $dt$ .

ties determined from the fundamental frequency analysis of the raw waveforms. The resulting velocity pattern in time (Fig. 5 bottom panel) also agrees qualitatively with the velocity values determined from the linear fits to the raw waveforms at the slip points. Comparison of the middle and bottom panels in Fig. 5 clearly shows that velocity increased during the intervals that  $P_{\text{el}}$  was at its upper bound, but was constant when  $P_{\text{el}}$  was at its lower bound.

To test energy conservation at the slip point, Eq. (2),  $F_{\text{sliding}}$  in Eq. (2) was calculated using the data of Fig. 5 and the dilation data of Fig. 4 (bottom panel) and compared to the viscous friction during sliding. The viscous friction during sliding was calculated from the component of sliding that occurred at the same frequency (1 Hz) as the input force, but  $90^\circ$  out of phase. Only this, the fundamental harmonic of the complex stick-slip response, contributes to energy loss.<sup>19</sup> The fit obtained by using a constant  $dt$  value of  $8 \mu\text{s}$  is shown in Fig. 6. The small value for  $dt$  indicates a relatively fast dilation process compared to the slip.

At velocities above  $500 \text{ \AA s}^{-1}$ , the viscous force decreased linearly with increasing velocity, as has often been supposed in theoretical models of stick-slip friction.<sup>22</sup> It may seem paradoxical that  $F$  decreases with  $v$  in this analysis, as it was either constant or increasing with  $v$  for data that this laboratory has published previously. There is no contradiction because the velocity range of Fig. 6 corresponds to the lowest accessible velocities in the stick-slip regime very close to the transition to sticking state. At sliding velocity larger than  $900 \text{ \AA s}^{-1}$ , steady state response is reached and the friction force is independent of the velocity, as we reported elsewhere.<sup>5,19,20</sup> Note that this behavior is to be distinguished from that observed for the sliding of rough surfaces, where kinetic friction often increases logarithmically with increasing velocity.<sup>23</sup> This study concerns a simpler model system where the surfaces were atomically smooth.

Increase of the friction force with velocity between 400 and  $500 \text{ \AA s}^{-1}$  can be related to the additional energy that the system requires to dilate. This suggests that dilation precedes slip and causes  $k_{\text{liquid}}$  to decrease at constant applied force.

Observations of granular friction indicate that vertical displacement reaches its maximum before the maximum in slip velocity.<sup>7,8</sup> Molecular dynamics simulations<sup>10,24</sup> similarly suggest that dilation begins prior to slip. Furthermore, studies of the yield point of organic glasses in the bulk show it to increase in proportion to the applied pressure,<sup>25,26</sup> which again suggests explanation in terms of volume expansion against a confining pressure. Although, taken together, these considerations suggest that it is actually the dilatancy that determines the magnitudes of static and kinetic friction, rather than the other way around, more experiments with other systems and a wider parameter space are needed before this hypothesis can be tested conclusively.

In extending this work it will be very interesting to contrast time-resolved changes of friction and dilatancy during the course of individual stick-slip cycles. In an earlier MD calculation it was observed to start at the edge of the contact region and propagate rapidly inwards.<sup>27</sup> Unfortunately at this point we do not have the lateral resolution needed to compare to this prediction, and it is not yet technically feasible (due to the very small amplitude of dilatancy oscillations) to acquire real-time measurements of dilatancy during the course of a single stick-slip cycle. However, looking to the future, it has been suggested that coupling between forces in orthogonal directions may afford methods to control the magnitude of friction.<sup>13-15</sup> This quantitative investigation of their relation has a bearing on quantifying the underlying mechanisms.

In summary, the coupling between friction (shear) response and volume change of a molecularly thin lubricant film confined between two solid surfaces has been experimentally observed for the first time, and the data are shown to be consistent with a simple model of energy balance between a small number of contributing components.

## ACKNOWLEDGMENTS

This work was supported by the U.S. Department of Energy, Division of Materials Science under Grant No. DEFG02-91ER-45439 to the Frederick Seitz Materials Research Laboratory at the University of Illinois at Urbana-Champaign. For travel assistance, we are grateful to TUBITAK (in Turkey) and to the U.S. National Science Foundation (International Programs).

<sup>1</sup>O. Reynolds, *Philos. Mag.* **20**, 469 (1885).

<sup>2</sup>J. Happel and H. Brenner, *Low Reynolds Number Hydrodynamics* (Martinus Nijhoff, The Hague, 1983).

<sup>3</sup>B. Bhushan, J. N. Israelachvili, and U. Landman, *Nature (London)* **374**, 607 (1995).

<sup>4</sup>A. L. Demirel and S. Granick, *Phys. Rev. Lett.* **77**, 2261 (1996); *J. Chem. Phys.* **115**, 1498 (2001).

<sup>5</sup>A. L. Demirel and S. Granick, *J. Chem. Phys.* **109**, 6889 (1998).

<sup>6</sup>J. Klein, *J. Non-Cryst. Solids* **235**, 422 (1988).

<sup>7</sup>S. Nasuno, A. Kudrolli, A. Bak, and J. P. Gollub, *Phys. Rev. E* **58**, 2161 (1998).

<sup>8</sup>J. Geminard, W. Losert, and J. P. Gollub, *Phys. Rev. E* **59**, 5881 (1999).

<sup>9</sup>C. J. Yu, A. G. Richter, A. Datta, M. K. Durbin, and P. Dutta, *Phys. Rev. Lett.* **82**, 2326 (1999).

<sup>10</sup>P. A. Thompson, G. S. Grest, and M. O. Robbins, *Phys. Rev. Lett.* **68**, 3448 (1992).

<sup>11</sup>M. Schoen, D. J. Diestler, and J. H. Cushman, *Phys. Rev. B* **47**, 5603 (1993).

- <sup>12</sup>L. V. Woodcock, Chem. Phys. Lett. **111**, 455 (1984).
- <sup>13</sup>J. Gao, W. D. Luedtke, and U. Landman, J. Phys. Chem. B **102**, 5033 (1998).
- <sup>14</sup>M. Heuberger, C. Drummond, and J. Israelachvili, J. Phys. Chem. B **102**, 5038 (1998).
- <sup>15</sup>V. Zaloj, M. Urbakh, and J. Klafter, Phys. Rev. Lett. **82**, 4823 (1999).
- <sup>16</sup>A. Dhinojwala, S.-C. Bae, and S. Granick, Tribol. Lett. **9**, 55 (2000).
- <sup>17</sup>C. Drummond and J. Israelachvili, Macromolecules **33**, 4910 (2000).
- <sup>18</sup>S. Granick, A. L. Demirel, L. Cai, and J. Peanasky, Israel J. Chem. **35**, 75 (1995).
- <sup>19</sup>G. Reiter, A. L. Demirel, and S. Granick, Science **263**, 1741 (1994); G. Reiter, A. L. Demirel, J. Peanasky, L. Cai, and S. Granick, J. Chem. Phys. **101**, 2606 (1994).
- <sup>20</sup>A. L. Demirel and S. Granick, Phys. Rev. Lett. **77**, 4330 (1996).
- <sup>21</sup>C. Drummond and J. Israelachvili, Phys. Rev. E **63**, 041506 (2001).
- <sup>22</sup>B. N. J. Persson, *Sliding Friction: Physical Principles and Applications*, 2nd ed. (Springer, New York, 2000).
- <sup>23</sup>T. Baumberger, P. Berthoud, and C. Caroli, Phys. Rev. B **60**, 3928 (1999).
- <sup>24</sup>Y. Zhang and C. S. Campbell, J. Fluid Mech. **237**, 541 (1992).
- <sup>25</sup>S. Bair and W. O. Winer, Trans. ASME, J. Tribol. **114**, 1 (1992).
- <sup>26</sup>Y. L. Chen, R. G. Larson, and S. S. Patel, Rheol. Acta **33**, 243 (1994).
- <sup>27</sup>B. N. J. Persson, J. Chem. Phys. **113**, 5477 (2000).